colloids and interfaces

MDPI

Article

What Can You Learn about Apparent Surface Free Energy from the Hysteresis Approach?

Konrad Terpiłowski [1,*], Lucyna Hołysz [1], Michał Chodkowski [1] and David Clemente Guinarte [2]

[1] Department of Interfacial Phenomena, Institute of Chemical Sciences, Faculty of Chemistry, Maria Curie Skłodowska University, M. Curie Skłodowska Sq. 3, 20-031 Lublin, Poland; lucyna.holysz@umcs.pl (L.H.); michal@chodkowski.eu (M.C.)

[2] Participant of a Research Project under the Erasmus Program, Faculty of Chemistry, Institute of Chemical Sciences, Maria Curie Skłodowska University, M. Curie Skłodowska Sq. 3, 20-031 Lublin, Poland; clemente.guinarte.david@gmail.com

* Correspondence: terpil@umcs.pl

Abstract: The apparent surface free energy is one of the most important quantities in determining the surface properties of solids. So far, no method of measuring this energy has been found. The essence of contact angle measurements is problematic. Contact angles should be measured as proposed by Young, i.e., in equilibrium with the liquid vapors. This type of measurement is not possible because within a short time, the droplet in the closed chamber reaches equilibrium not only with vapors but also with the liquid film adsorbed on the tested surface. In this study, the surface free energy was determined for the plasma-activated polyoxymethylene (POM) polymer. Activation of the polymer with plasma leads to an increase in the value of the total apparent surface free energy. When using the energy calculations from the hysteresis based approach (CAH), it should be noted that the energy changes significantly when it is calculated from the contact angles of a polar liquid, whereas being calculated from the angles of a non-polar liquid, the surface activation with plasma changes its value slightly.

Keywords: hysteresis approach; plasma; POM

Citation: Terpiłowski, K.; Hołysz, L.; Chodkowski, M.; Clemente Guinarte, D. What Can You Learn about Apparent Surface Free Energy from the Hysteresis Approach?*Colloids Interfaces* **2021**, *5*, 4. https://doi.org/10.3390/colloids5010004

Received: 27 October 2020
Accepted: 29 December 2020
Published: 14 January 2021

1. Introduction

The apparent surface free energy of solids is a quantity that cannot be determined directly for most surfaces. The literature [1] reports a number of theoretical approaches used to calculate this quantity, mainly based on the measurement of contact angles. Currently, the methodology of measuring contact angles is widely discussed in the literature [2–4]. In this paper, the problem of apparent surface free energy is considered on the basis of a plasma-activated (POM) polymer. The plasma was obtained from various gases (air, oxygen, argon and nitrogen). The apparent surface free energy of the tested materials was determined from the approach proposed by Chibowski (CAH) [5,6] (Equation(1)) based on the hysteresis of contact angles.

$$\gamma_s = \frac{\gamma_l (1+\cos\theta_a)^2}{(2+\cos\theta_r+\cos\theta_a)} \quad (1)$$

where γs—the surface free energy, γ_l—the liquid surface tension, θ—the advancing contact angle, θ_r—the receding contact angle

The obtained values are compared with those calculated from the Good, van Oss and Chaudhury (LWAB) (Equation(2,3)) approach [7–9],

$$\gamma_s = \gamma_s^{LW} + \gamma_s^{AB} \quad (2)$$

$$\gamma_s^{AB} = 2\left(\gamma_s^+ + \gamma_s^-\right)^{0.5} \quad (3)$$

where γ_s—the surface free energy, γ_s^{LW}—the Lifshitz-van der Waals component, γ_s^{AB}—the acid-basis component, γ_s^+—the acid component, γ_s—the base component.

As was mentioned above, the most common method used for surface free energy determination is the contact angle measurements of solids. From a thermodynamic point of view, the system where the contact angle is measured contains solid, vapor and liquid phases. However, the thermodynamic aspects are quite problematic for defining and determining the surface free energy of solids. In fact, in these systems, interfaces such as solid–vapor, solid–liquid, liquid–vapor or solid–liquid–vapor are also present. These additional interfaces are often not considered or are approximated as sharp transitions with a discontinuity in the physical properties because the exact mathematical description of them is impossible due to discontinuities and the unknown thicknesses of the transition region [10]. One of the approximations that can be useful for the description of these systems is the Gibbs ideal interface model (the so-called dividing surface approximation or D-face) which assumes that three-phase contact for a sessile drop corresponds to the intersection line of the undisturbed two-phase interfaces (D-face) and can be described by Laplace equations (basic and generalized) [11]. This thermodynamic model proposes surface (interface) energy as the aggregate of the surface tension and the sum of the product of the chemical potential and the absolute absorption of every compound of the system. It also explains why there is no equality sign between surface free energy and surface tension, even in a one-compound system.

In addition, it must be kept in mind that the equilibrium contact angle (in a thermodynamic sense, resulting from Young's equation) is immeasurable and that the contact angle, which is measured directly, is referred to as the "apparent" contact angle due to restrictions mentioned above. Because of this, there are various methods and techniques proposed in the literature to improve the accuracy and precision of the contact angle measurements.

The research on the effect of plasma on the wettability of polymers is one of the main topics studied at the Department of Interfacial Phenomena [12–14]. The research presented in the paper covers the influence of various activations of (POM) polymer surface with plasma obtained from air, oxygen, argon and nitrogen. (POM) can be used as an anti-adhesive, anti-corrosive, anti-friction material and for the production of high-strength components in vehicles, household appliances, automation and control devices. The aim of this paper is to examine all potentialities of the equation based on the hysteresis of contact angles [5,6] for the apparent surface free energy estimation.

2. Materials and Methods

2.1. Sample Preparation

The first stage of preparation of polymer plates for testing included preparation of plates, polyoxymethylene (POM) (Plastic Group Polska) (Figure 1), 1 × 2 cm in size from a larger plate. Then, the obtained plates were washed in an aqueous detergent solution (Extran MA 02, Merck, Germany) and rinsed with distilled water. The plates were then washed in a methanol/water (1:1) solution for 15 min in an ultrasonic bath and rinsed with distilled water. The samples prepared in this way were dried in an oven at 40 °C for 1 h and kept in a desiccator before measurements.

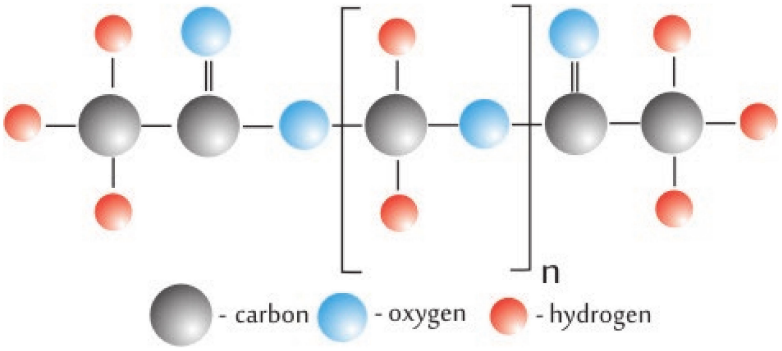

Figure 1. POM polymer model idealized molecule [15].

2.2. Plasma Activation

Modification of polymer and glass surfaces with low-pressure plasma with a power of 400 W was carried out with the use of a Pico apparatus, Diener Electronic, (Ebhausen Germany). The plates were placed on a shelf in a special chamber of the apparatus. The surface modification process with the plasma generated in various gases was carried out at a pressure of 0.2 mbar with a gas flow of 22 cm^3/min for a specified time. Then, air was blown through to remove gaseous products accumulated in the chamber, and the pressure was equalized to atmospheric pressure, which allowed the measurement chamber to be reopened.

2.3. Contact Angle Measurements

The contact angles of the tested liquids of water (Milli-Q 185, Merck, Darmstadt, Germany) and diiodomethane (M = 267.84 g/mol, 99%, Sigma Aldrich, Steinheim, Germany) were measured with a GBX (Digidrop, Romans sur Isere, France) apparatus with humidity control, using the Windrop ++ software. The polymer plates were placed in the chamber of the apparatus thermostatted to 20 °C and 50% RH in the chamber. The liquid whose contact angles were also measured was thermostatted to 20 °C by connecting a contact angle measuring apparatus to a thermostat (Lauda RE 104, Königshofen Germany). The droplets with a capacity of 6 μL were placed on the surface to measure the advancing contact angles, and the droplet volume was reduced to 4 μL to measure the receding contact angles. The software measured the contact angles to the right and left of the droplet and automatically took the average of the measurements. Indication of droplet baseline, three-phase contact points and height of the examined droplet was necessary. Based on these, using the polynomial algorithm and the NURBS (non-uniform rational basis spline) model, the program computed the contact angle. The presented results were obtained from at least 10 measurements. Air, oxygen, argon and nitrogen (Air Products, Siewierz, Poland) were used for activation.

2.4. Optical Profilometry

The surface roughness was tested with the Contour GT optical profilometer from (Bruker, Karlsruhe, Germany). This method uses a laser beam, which gives non-contact and non-invasive measurements. They are based on the measurement of the distance between the white light or the laser beam emitter and the tested surface, which is possible owing to the knowledge of the difference between the exit time and the input of the incident beam. For the surface characterization, the following roughness parameters were calculated:

- the arithmetic mean deviation of the profile from the mean line, measured along the measuring or elementary section: Ra;
- the Root Mean Square deviation standard from the vertical mean value of measurement coordinates: *Rq*;
- the distance between the deepest valley and the highest elevation: *Rt*
- Roughness parameters were calculated using WYKO—Vison software, and the 3d images were obtained using GWYDDION software.

2.5. Infrared Spectroscopy (IR-ATR)

The IR-ATR spectra were made using a Thermo Scientific, Nicolet iS10 spectroscope (Warsaw, Poland) (diamond crystal). The background spectrum was obtained first. Then, the spectra of the polymer samples were made; each spectrum is the result of 32 scans. The raw spectra were processed with Omnic-9 software. In order to compare the obtained results, the common scale function was used for all spectra.

2.6. X-ray Photoelectron Spectroscopy (XPS)

The plates on which XPS tests were performed were activated with plasma just before insertion into the spectroscope. They were transported in separate vessels, ensuring that

the packaging material did not touch the top layer. The spectra were obtained using the UHV multi-chamber analytical system by Prevac sp.z o.o. (Rogów, Poland).

3. Results and Discussion

As shown in Figure 2, the advancing contact angle of water is 87.9° ± 5.5, and the receding angle is 55.5° ± 6.2. Plasma activation of the surface contributes to a significant decrease in the value of the contact angle. In the case of surface activation with plasma obtained from oxygen, air and nitrogen, the ascending angle is approximately 63°. Even greater modification is observed when the argon plasma is used to activate the surface, as the ascending angle drops to 40.5° ± 7.6. The ascending contact angle of water on POM was measured by Relyon Plasma, Germany being 73.5° on the unmodified polymer [16], and 5 min. after activation with atmospheric plasma, it was 57.5°. The value of the rising contact angle depends on many factors: polymer composition, chemical heterogeneity and roughness. Plasma activation leads to smoothing and unification of the surface. This effect is visible in the experiment comparison: the ascending angle differs by about 10°, while the receding angle is practically identical.

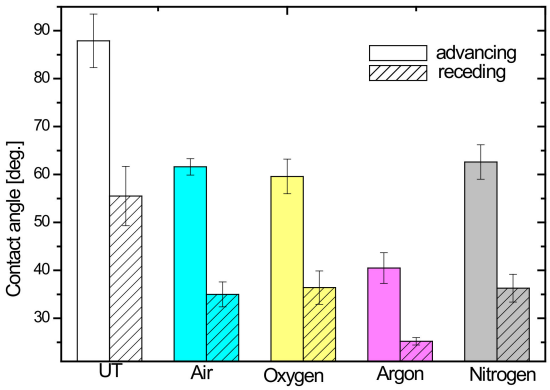

Figure 2. Advancing and receding contact angles of water measured on the unmodified and modified plasma.

Diiodomethane and glycol contact angles (not shown here) were also measured in order to test all the possibilities offered by the hysteresis contact angle approach. As can be seen in Figure 3, the diiodomethane contact angle does not change as much as the water contact angle. In most cases, the change in value is within the standard deviation between the cases. Only in the case where the plasma is obtained from oxygen, the contact angle increased by around 10°.

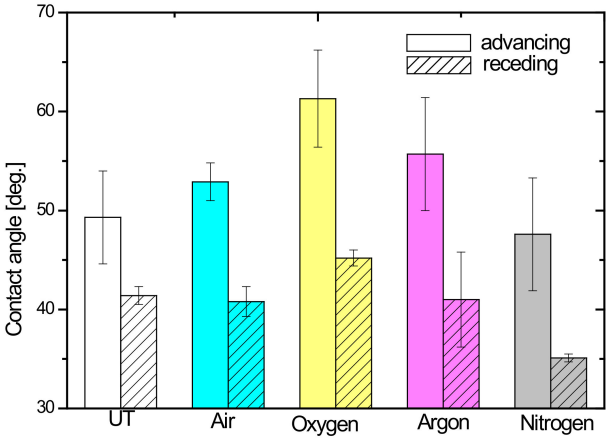

Figure 3. Advancing and receding contact angles diiodomethane measured on unmodified and modified plasma.

The value of the calculated apparent surface free energy is the resultant of surface roughness and chemistry. Comparing the total value of apparent surface free energy, it can be seen that the activation of the polymer surface with plasma changes the value of surface free energy. Getsche et al. [17] activated the POM surfaces using a plasma gun and oxygen as plasma gas, for calculation of apparent surface free energy by applying the Owens—Wendt approach [18].(Equation (4))

$$\gamma_l(1+\cos\theta) = 2(\gamma_s^d\gamma_l^d)^{1/2} + 2(\gamma_s^p\gamma_l^p)^{1/2} \quad (4)$$

where γ_l—the surface tension of the test liquid, θ—the contact angle, $\gamma_s{}^d$—the solid dispersive component, $\gamma_s{}^p$—the solid polar component, $\gamma_l{}^d$—the liquid dispersive component, $\gamma_l{}^p$—the liquid polar component

The total value of energy is higher by about 4 mJ/m^2 in comparison with our experiment. However, this approach always gives higher values in comparison with the other approaches, which we discussed in the manuscript [19]. However, when the difference between the nonactivated and activated samples takes into account the energy of the plasma-treated sample being about 5 mJ/m^2 higher, it is fully consistent with the results of our experiment. In the case of the energy calculated from the hysteresis approach presented as an average of three test liquids, it can be seen that the energy increases when the contact angles are measured on the plasma-activated plates (Table 1). The largest increase was observed when argon was the plasma gas. In the case of using the LWAB [19] approach to calculate energy, it is difficult to notice a clear trend of energy changes. Water, diiodomethane and ethylene glycol were used to measure the contact angles to calculate the apparent surface free energy from the LWAB [19] equation. Our earlier research on the PEEK polymer [18] shows that it is not possible to use formamide to measure contact angles, especially when the plasma was obtained from nitrogen. The formamide was completely spread over with the surface. Using the LWAB [19] approach to calculate the total apparent surface energy in this case, it can only be said that there were changes induced at the surface by the action of the plasma. The apparent surface free energy consists of interactions of a dispersive and polar nature [19]. Liquids interact with the surface in the same way; therefore, nonpolar liquids can be used to calculate the nonpolar component of the apparent surface free energy. Therefore, the apparent surface free energy calculated from the CAH [20–22] approach was compared using the diiodomethane [13,23] contact angles, whose surface tension was 50.8 mJ/m^2, with the dispersion component calculated from the CAH [24,25] approach. Changes in the dispersion component for individual types of surfaces are practically within the standard deviation. Thus, it can be concluded that plasma does not affect the dispersion component of apparent surface free energy. When comparing the values using the two approaches, it should be noted that by applying the hysteresis approach, larger values of the total energy and the dispersion component are obtained. This is due to the fact that for calculating the energy from the CAH approach, one can use both the advancing and receding angles, while in the second approach under consideration, only the advancing angle should be used, as intended by the authors. The hysteresis approach takes into account the obtained results and the influence of topography and surface chemistry. Going further, you can compare the component of polar interactions with the value of the difference in energy calculated from CAH for water and diiodomethane. If diiodomethane interacts with the surface in a non-polar manner and the surface tension of the water can be divided into a dispersion element of 21.8 mJ/m^2 and a polar element of 51.0 mJ/m^2, the calculation of such a difference may allow for the estimation of polar interactions on the surface. Comparing these values, it can be seen that the polar interactions increase when the surface is activated with plasma. There are some imperfections in both approaches, e.g., failure to calculate the polar component from the CAH approach on the surface of the starting polymer. This is most likely due to the fact that water has only 21.8 mJ/m^2 of dispersion interactions, while on the actual polymer surface, they are greater; using only water contact angles and the CAH approach

for energy estimation in this case would result in an underestimation of the energy value. However, in the case of the LWAB approach, it was not possible to calculate the polar component for the argon plasma-activated surface because the square root of the γ^+ parameter from the calculations has a negative value, which is impossible from a physical point of view. Summing up the obtained results, it can be seen that the polar interactions change as a result of plasma activation of this polymer, while, knowing the chemical nature of solids [25,26], even when taking into account only the hysteresis approach, it can be assumed that electron donor interactions change. The biggest change can be seen when argon is used as the plasma gas because argon has the largest particles and its impact on surfaces is the most effective.

Table 1. Apparent surface free energy calculated from the CAH and LWAB approaches.

Sample	$\gamma^{tot}_{CAH(W,DM,G)}$	$\gamma^{tot}_{CAH(W)}$	$\gamma^{tot}_{CAH(DM)}$	$\gamma^{tot}_{CAH(W)} - \gamma^{tot}_{CAH(DM)}$	$\gamma^{tot}_{LWAB(W,DM,G)}$	γ_{LW}	γ^-	γ^+	γ^{AB}
UT	38.1 ± 4.0	37.1 ± 5.8	42.5 ± 2.2	-	36.0 ± 2.8	34.6 ± 3.7	6.7 ± 7.0	0.3	2.1 ± 1.4
Air	42.9 ± 4.5	48.8 ± 1.7	40.5 ± 3.2	7.6 ± 1.5	38.7 ± 2.5	36.6 ± 3.4	22.2 ± 0.6	0.4	6.0 ± 1.4
Oxygen	42.6 ± 6.5	49.9 ± 2.9	40.7 ± 4.7	9.1 ± 1.8	33.2 ± 3.0	27.8 ± 2.8	30.2 ± 1.5	0.2	5.3 ± 0.2
Argon	44.6 ± 4.0	61.4 ± 4.5	38.9 ± 4.7	22.5 ± 0.2	31.0 ± 3.3	31.0 ± 3.3	68.4 ± 3.6	-	-
Nitrogen	42.1 ± 4.0	47.5 ± 2.7	41.1 ± 3.3	6.4 ± 0.6	37.0 ± 3.8	35.6 ± 3.1	23.6 ± 0.9	0.03	1.5 ± 0.6

W—water, DM—diiodomethane, G—glycol [mJ/m^2], tot—total value of apparent surface free energy, +—index relating to the electron-acceptor parameter of the apparent surface free energy, −—index relating to the electron-donor parameter of the apparent surface free energy, AB—acid-base component of apparent surface free energy.

By analyzing the obtained IR-ATR spectra, one can see characteristic vibration bands for the wavelength of 2923 cm^{-1}, which corresponds to the asymmetric stretching vibrations of the CH_2-O groups (Figure 4). Another visible band of vibrations corresponds to the wavelength of 1236 cm^{-1}, corresponding to the symmetrical vibrations of the CH_2 group. For the 1089 cm^{-1} wavelength, there is a characteristic peak for the asymmetric stretching vibrations of the C-O-C groups, and as can be seen from Figure 4, it is this type of vibration that is mostly influenced by the activation of the polymer surface with plasma. The peak present at a wavelength of 886 cm^{-1} corresponds to the symmetrical C-O-C absorption stretching vibrations. Observing the effect of plasma on the change of the chemical properties of the POM surface, a certain dependence was found in comparison with the spectrum of the polymer not treated with plasma. In the case when oxygen was used for excitation, all peaks characteristic of individual groups are much higher. Nitrogen plasma modifies the surface to the smallest extent. If the information obtained from the IR spectra is combined with the results of the measured contact angles (Figures 2 and 3) and the calculated apparent surface free energy (Figure 3), the greatest increase in the surface energy is found when the surface is activated with argon plasma. In the case of plasma obtained from oxygen, a large change of contact angles of diiodomethane corresponds to the change of dispersion component of surface free energy. The analysis of the IR spectra allowed for the selection of samples for the more profound analysis using the XPS technique.

During the cold plasma process, electromagnetic radiation in a wide range from IR (heat) to UV and vacuum UV also appears. The generated UV radiation is strong enough to break bonds in the structure of the modified material. In addition, while oxygen plasma is generated, the reactive oxygen species (ROS) such as superoxide, singlet oxygen and hydroxyl radicals are also formed [27]. Both of these factors can lead to changes in the polymer chain similar to thermal oxidation and photooxidation. Although photodegradation may occur in the absence of oxygen, it is significantly accelerated by its various forms. Because the plasma modification affects only the surface layer of the material, this explains the decrease in the share of aliphatic sp^3 carbons in species such as ≡C-H and ≡C-C≡ derived from the polymer chain in favor of epoxide (=C-O-C=), hydroxyl (≡C-O-H) or carbonyl (=C=O) groups, which can be observed from the XPS analysis (Tables 2 and 3).

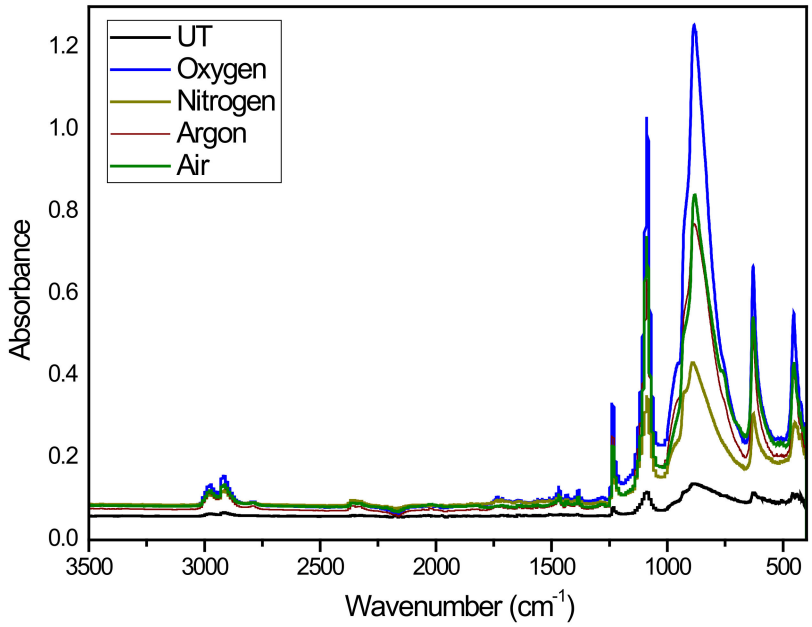

Figure 4. IR ATR spectra of untreated and plasma-treated POM.

Table 2. XPS data C1s obtained for the untreated and plasma-treated samples.

Species	UT	Argon Plasma	Oxygen Plasma
C-O-C (main POM molecular unit)	40.6	36.3	36.7
C-O-C (epoxy groups)	7.2	14.9	14.3
C-H sp3 (aliphatic carbon)	6.6	3.8	4.0
C-C sp3 (aliphatic carbon)	12.3	4.0	5.0
C=O (carbonyl group)	11.7	14.8	14.7

% Atomic Concentration.

Table 3. XPS data O1s obtained for untreated and plasma-treated samples.

Species	UT	Argon Plasma	Oxygen Plasma
C-O-C (main POM unit)	61.3	61.8	65.4
OH-C (hydroxyl groups bound to aliphatic carbon)	9.8	8.8	10.4
O-C=O (carboxyl groups)	26.6	24.5	23.1

% Atomic Concentration.

In the case of oxygen plasma modification (Figure 5), the oxidation mechanism proposed by Chai et al. [28] can be adapted to describe the changes induced on the POM surface. Accordingly, the singlet oxygen ($^1O_2$) (Table 3) and the atomic oxygen O(^{3}P) resulting from the plasma generation are expected to be the main molecular entity that reacts with the polymer surface. From the exemplary oxidation schemes, it can be concluded that carboxyl, carbonyl and carbonate groups will be formed, which is confirmed by the XPS analysis.

One of the methods for chemical activation of plastic is the usage of noble gas plasma, such as argon plasma [29–31]. Argon molecules can be excited or ionized, and their reactivity is very high. They are able to remove electrons from chemical bonds, resulting in the generation of open bonds (radicals). Some of the possible reactions of argon plasma with the POM surface are shown (Figure 5).

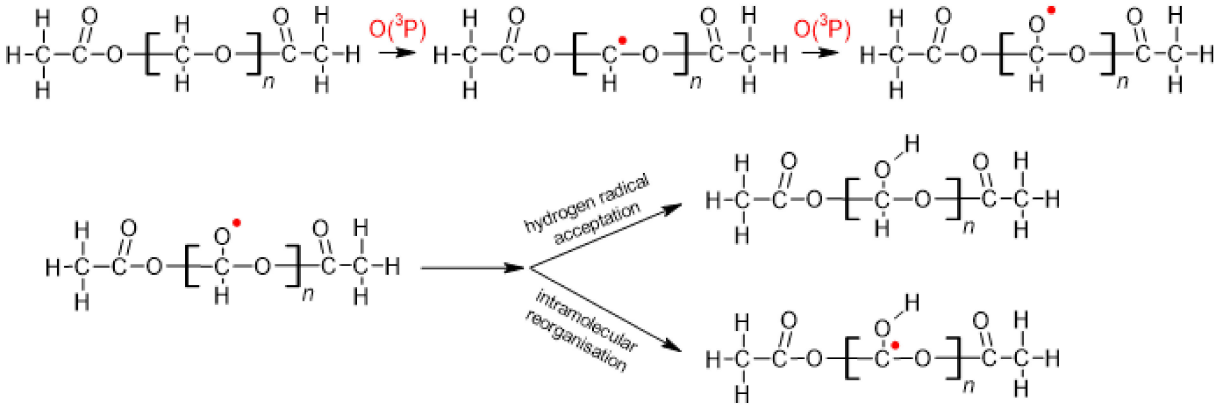

Figure 5. Exemplary diagram of the POM surface oxidation as a result of oxygen plasma modification.

Effects of argon (Figure 6) ions or UV radiation can also break other bonds, such as C-C and C-O-C. However, the data from XPS O 1s spectrum show that there are no significant differences in the concentration of oxygen atoms from the POM units. Moreover, the data from the C 1s (Table 2) spectrum confirm that the amount of C-H species decreased, which confirms oxidation of these groups (in the case of oxygen plasma modification) or active site creation (in the case of argon plasma modification). Thus, it can be concluded that the C-O-C bonds in the main POM unit are not broken and breaking the C-H bonds in this case is privileged. However, the differences in the aliphatic (sp^3) C-C carbon concentrations indicate the possibility of breaking these bonds at the ends of the polymer, where the chain termination is observed (Table 2).

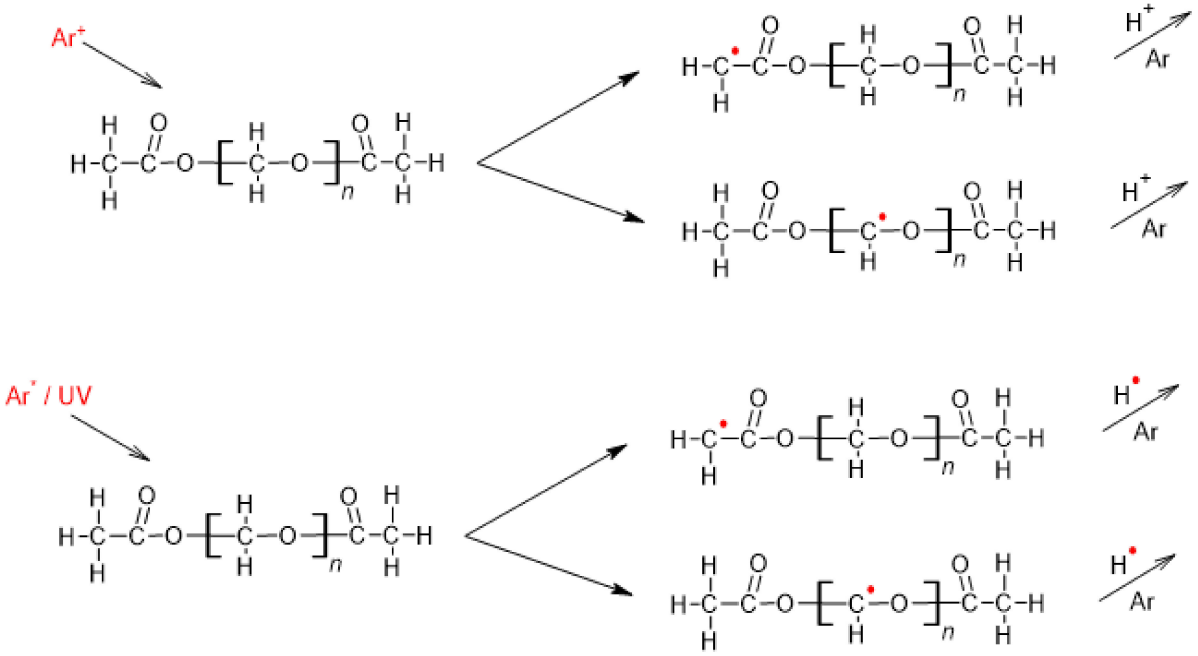

Figure 6. Action of argon plasma on the POM surface.

Similar to the case of oxygen plasma, the changes occurring as a result of argon plasma treatment, despite the lack of oxygen during the process, can be explained by the reactions on the polymer surface after contact with atmospheric air. It must be kept in mind that in the final stage of plasma treatment, the reaction chamber is flushed with atmospheric air, which gets directly to the activated surface. In the case of the argon plasma process, further reactions that are taking place due to the ingress of atmospheric oxygen seem to be similar to those during activation with oxygen plasma. Nevertheless, they will

occur with less efficiency. Only in the case of modification with oxygen plasma is there a greater concentration of -OH groups on the surface because the hydroxyl radical is directly accessible in the reaction medium.

Activation of the POM surface with plasma reduces the surface roughness. As can be seen in the 3D images presented in Figure 7, the surface of the tested polymer is rough on the micrometric scale. As a result of the treatment, longitudinal indentations were formed on the surface of the polymer, and mounds with additional irregular roughness can be seen between the indentations. The scale of the z axis in Figure 7A is the largest because the untreated surface has the highest value of the Rq parameter (Table 4). The plasma obtained from air, oxygen and argon reduces the roughness in a comparable manner, while this effect is less visible when nitrogen-based plasma gas was used for activation.

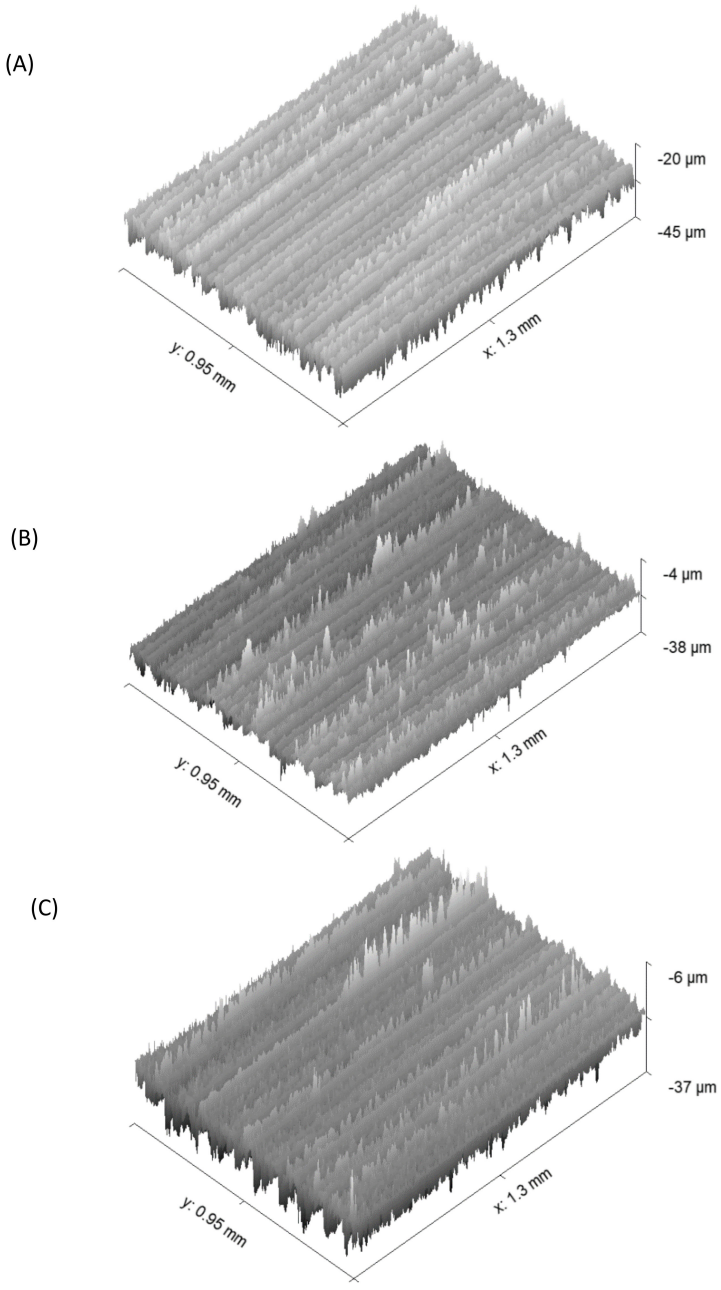

Figure 7. *Cont.*

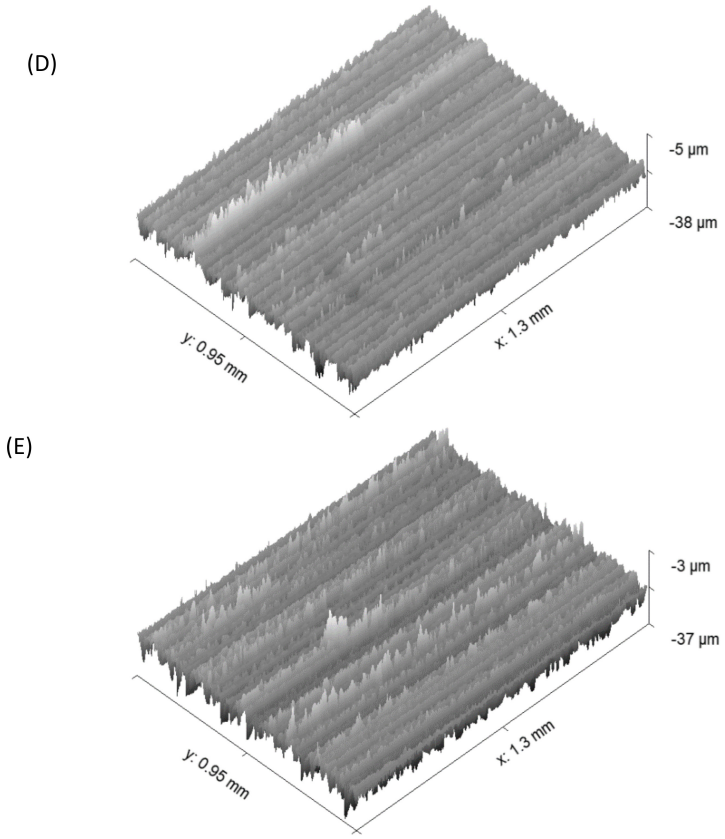

Figure 7. 3D images obtained by the optical profilometry.

Table 4. POM surface roughness parameters of the unmodified and plasma-modified surfaces.

	R_a	R_q	R_t
UT	2.6 ± 0.4	3.3 ± 0.4	32.8 ± 7.3
Air	2.1 ± 0.4	2.7 ± 0.4	30.8 ± 5.8
Oxygen	2.2 ± 0.2	2.9 ± 0.1	34.6 ± 3.7
Argon	2.2 ± 0.01	2.9 ± 0.02	34.0 ± 1.4
Nitrogen	2.5 ± 0.1	3.2 ± 0.1	32.9 ± 1.2

R_a—average roughness, R_q—square mean of the surface roughness, R_t—maximum. roughness height. Parameters are listed in µm.

4. Conclusions

Surface activation with plasma increases the value of apparent surface free energy. This is due to a change in the chemical groupings on the surface, evidence of which can be found in the IR and XPS studies. Moreover, the activation of the surface with plasma leads to the uniformity of the surface by reducing the roughness. The change in surface properties is caused by an increase in the value of the electron-donor parameter of the energy. As shown by XPS tests, the change of this parameter is due to a decrease in the number of C-H groups on the surface and bonds between carbon atoms.

Taking into account both approaches used for calculating the apparent surface free energy, it should be noted that both give comparable results in terms of the total value of apparent surface free energy. Reconsidering Young assumptions, it seems that the value from the hysteresis approach is closer to the real value of energy. In the literature, the term "apparent" is often used with regard to the surface energy. As can be seen from the comparison of the energy calculated with CAH from water and diiodomethane angles, such a definition is correct. Using even two polar and non-polar liquids from the hysteresis-

based approach, it is possible to obtain a lot of valuable information, not only about the total apparent surface free energy value but also its polar component.

Author Contributions: K.T.: author of the concept of the work, carrying out plasma activation of the surface, calculation of the apparent surface free energy, execution and analysis of the IR ATR results; L.H.: development of profilometric data; M.C.: development of XPS results, preparation of potential mechanisms of plasma-polymer reaction; D.C.G.: measurement of contact angles and statical analysis of the obtained results. All authors have read and agreed to the published version of the manuscript.

Funding: The research was financed by a subsidy of the Ministry of Education and Higher Education of the Republic of Poland. The participation of David Clemente Guitare was financed by the Erasmus academic exchange program.

Data Availability Statement: Data sharing not applicable. The manuscript contains original scientific research not previously published anywhere.

Conflicts of Interest: The authors declare no conflict of interest.

References

1. Żenkiewicz, M. Methods for the calculation of surface free energy of solids. *J. Achiev.* **2007**, *24*, 137–145.
2. Drelich, J.W.; Boinovich, L.; Chibowski, E.; Della Volpe, C.; Hołysz, L.; Marmur, A.; Siboni, S. Contact angles: History of over 200 years of open questions. *Surf. Innov.* **2020**, *8*, 3–27. [CrossRef]
3. Chibowski, E. On some relations between advancing, receding and Young's contact angles. *Adv. Colloid Interface Sci.* **2007**, *133*, 51–59. [CrossRef] [PubMed]
4. Bormashenko, E. Apparent contact angles for reactive wetting of smooth, rough, and heterogeneous surfaces calculated from the variational principles. *J. Colloid Interface Sci.* **2019**, *537*, 597–603. [CrossRef] [PubMed]
5. Chibowski, E. Contact angle hysteresis due to a film present behind the drop. In *Contact Angle, Wettability and Adhesion*, 2nd ed.; Mittal, K.L., Ed.; VSP: Utrecht, The Netherlands, 2002; Volume 2, pp. 265–288.
6. Chibowski, E. On the interpretation of contact angle hysteresis. *J. Adhes. Sci. Technol.* **2002**, *16*, 1367–1404. [CrossRef]
7. van Oss, C.J.; Good, R.J.; Chaudhury, M.K. The role of van der Waals forces and hydrogen bonds in "hydrophobic interactions" between biopolymers and low energy surfaces. *J. Colloid Interface Sci.* **1986**, *111*, 378–390. [CrossRef]
8. van Oss, C.J.; Good, R.J.; Chaudhury, M.K. Additive and nonadditive surface tension components and the interpretation of contact angles. *Langmuir* **1988**, *4*, 884–891. [CrossRef]
9. van Oss, C.J.; Good, R.J.; Chaudhury, M.K. Interfacial Lifshitz-van der Waals and polar interactions in macroscopic systems. *Chem. Rev.* **1988**, *88*, 927–941. [CrossRef]
10. Schmitt, M.; Heib, F. High-precision drop shape analysis on inclining flat surfaces: Introduction and comparison of this special method with commercial contact angle analysis. *J. Chem. Phys.* **2013**, *139*, 1–10. [CrossRef]
11. Schmitt, M.; Heib, F. More Appropriate Procedure to Measure and Analyse Contact Angles/Drop Shape Behaviours. In *Advances in Contact Angle, Wettability and Adhesion*, 3rd ed.; Mittal, K.L., Ed.; Wiley-Scrivener: Beverly, MA, USA, 2018; Volume 3, pp. 3–57.
12. Perèz-Huertas, S.; Terpiłowski, K.; Tomczyńska-Mleko, M.; Mleko, S.; Szajnecki, Ł. Time-based changes in surface properties of poly(ethylene terephthalate) activated with air and argon-plasma treatments. *Colloids Surf. A Physicochem. Eng. Asp.* **2018**, *558*, 322–329. [CrossRef]
13. Rymuszka, K.; Terpiłowski, K.; Borowski, P.; Hołysz, L. Time-dependent changes of surface properties of polyether ether ketone caused by air plasma treatment. *Polym. Int.* **2016**, *65*, 827–834. [CrossRef]
14. Pèrez-Huertas, S.; Terpilowski, K.; Tomczyńska-Mleko, M.; Mleko, S. Surface modification of albumin/gelatin films gelled on low-temperature plasma-treated polyethylene terephthalate plates. *Plasma Process Polym.* **2020**, *3*, 1900171. [CrossRef]
15. Available online: https://omnexus.specialchem.com/selection-guide/polyacetal-polyoxymethylene-pom-plastic (accessed on 12 January 2021).
16. Available online: https://www.relyon-plasma.com/glossary/polyoxymethylene (accessed on 5 October 2020).
17. Gesche, R.; Kovacs, R.; Scherer, J. Mobile plasma activation of polymer using the plasma gun. *Surf. Coat. Technol.* **2005**, *200*, 544–547. [CrossRef]
18. Owens, D.K.; Wendt, R.C. Estimation of the surface free energy of polymers. *J. Appl. Polym. Sci.* **1969**, *13*, 1741–1747. [CrossRef]
19. Chibowski, E.; Terpiłowski, K. Comparison of Apparent Surface Free Energy of Some Solids Determined by Different Approaches. In *Contact Angle, Wettability and Adhesion*; Mittal, K.L., Ed.; CRC Press: London, UK, 2009; Volume 6, pp. 283–299.
20. Terpiłowski, K.; Wiącek, A.E.; Jurak, M. Influence of nitrogen plasma treatment on the wettability of polyetheretherketone and deposited chitosan layers. *Adv. Polym. Technol.* **2018**, *37*, 1557–1569. [CrossRef]
21. Fowkes, F.M. Attractive forces at interfaces. *Ind. Eng. Chem.* **1964**, *56*, 40–52. [CrossRef]
22. Terpiłowski, K.; Hołysz, L.; Chibowski, E. Surface free energy of sulfur—Revisited II. Samples solidified against different solid surfaces. *J. Colloid Interface Sci.* **2008**, *319*, 505–513. [CrossRef]

23. Jurak, M.; Chibowski, B. Surface free energy and topography of mixed lipid layers on mica. *Colloids Surf. B* **2010**, *75*, 165–174. [CrossRef]
24. Chibowski, E. Some problems of characterization of a solid surface via the surface free energy changes. *Adsorp. Sci. Technol.* **2017**, *35*, 647–659. [CrossRef]
25. Stammitti-Scarpone, A.; Acosta, E.J. Solid-liquid-liquid wettability and its prediction with surface free energy models. *Adv. Colloid Interface Sci.* **2019**, *264*, 28–46. [CrossRef]
26. Chibowski, E.; Perea-Carpio, R. Problems of contact angle and solid surface free energy determination. *Adv. Colloid Interface Sci.* **2002**, *98*, 245–264. [CrossRef]
27. Filipić, A.; Gutierrezi-Aguiree, I.; Primc, G.; Mozetič, M.; Dobnik, D. Cold Plasma, a New Hope in the Field of Virus Inactivation. *Trends Biotechnol.* **2020**, *38*, 1278–1291. [CrossRef] [PubMed]
28. Chai, J.; Fuzhi, L.; Li, B.; Kwok, D.Y. Wettability Interpretation of Oxygen Plasma Modified Poly(methyl methacrylate). *Langmuir* **2004**, *20*, 10919–10927. [CrossRef] [PubMed]
29. Karimian, D.; Yadollahi, B.; Zendehdel, M.; Mirkhani, V. Efficient dye-sensitized solar cell with a pure thin film of a hybrid polyoxometalate covalently attached organic dye as a working electrode in a cobalt redox mediator system. *RSC Adv.* **2015**, *5*, 76875–76882. [CrossRef]
30. Gernot, M.; Wallner, G.M.; Geretschläger, K.J.; Hintersteiner, I.; Buchberger, W. Characterization of polyoxymethylene for backsheets of photovoltaic modules. *J. Plast.* **2016**, *33*, 345–360.
31. Li, Y.; Zhou, T.; Chen, Z.; Hui, J.; Li, L.; Zhang, A. Non-isothermal crystallization process of polyoxymethylene studied by two-dimensional correlation infrared spectroscopy. *Polymer* **2011**, *52*, 2059–2069. [CrossRef]